Ultrafast spectroscopy of semiconductor saturable absorber mirror

Jing Zhang (张 靓)[1,2*], Dominik Bauer[2], Farina König[2], Thomas Dekorsy[2], Xihe Zhang (张喜和)[1], and Yafu Chen (陈亚符)[1]

[1] *Department of Physics, Changchun University of Science and Technology, Changchun 130022, China*

[2] *Department of Physics and Center of Applied Photonics, University of Konstanz, Konstanz, Germany*

[*] *E-mail: zhangj@cust.edu.cn*

Received January 26, 2010

Ultrafast spectroscopy of semiconductor saturable absorber mirror (SESAM) is measured using a femtosecond pump-probe experiment. This allows dynamic responses of SESAM in the cavity to be concluded by ultrafast spectroscopy. Change in reflection is measured as a function of pump-probe delay for different pump excitation fluences. Change of nonlinear reflection of SESAM is measured as a function of incident light energy density. When the excitation fluence increases, nonlinear change in ultrafast spectroscopy of SESAM becomes increasingly significant. When SESAM is pumped by an ultrahigh excitation fluence, the energy density of which is approximately 1400 μJ/cm^2, two-photon absorption can be observed visibly in its ultrafast spectroscopy.

OCIS codes: 140.7090, 140.4050, 320.7080.

doi: 10.3788/COL20100807.0676.

The first semiconductor saturable absorber mirror (SESAM), the breakthrough anti-resonant Fabry-Perot saturable absorber that first demonstrated a passively mode-locked Nd:YLF laser without Q-switching[1], was invented in 1992. Since then, SESAM has been acknowledged as the most promising mode-locking device. It has sparked the interest of various researchers across the globe[1,2].

As a reflecting mirror in the cavity, SESAM is responsible for passive mode-locking in ultrafast laser. Ultrafast dynamics of excited carriers inside SESAMs can directly influence the characteristics of output ultrashort pulses. Ultrafast dynamic processes are exceedingly short. Majority of these processes are too short to be observed using traditional measuring technologies, such as electronic techniques, because they are limited by temporal resolution. However, ultrafast lasers have advanced the temporal resolution of measurements into sub-10-fs regime, allowing for direct observation of ultrafast dynamics of excited carriers in SESAMs[3−5].

Femtosecond pump-probe technology is frequently applied in ultrafast spectroscopy detection. It makes real-time observation of ultrafast dynamics possible. This technique has been applied in studying saturation characteristics of SESAMs[6−10]. In our experiment, pump-probe setup was used for ultrafast spectroscopy detection of dynamic response of the SESAM at varying excitation fluences. When the excitation fluence increases, nonlinear change in ultrafast spectroscopy of the SESAM becomes increasingly significant[11,12]. In this letter, we reveal the nonlinear changes and provide a detailed explanation of the generation mechanism of nonlinear changes in ultrafast spectroscopy.

The sample used in the experiment—low-loss SESAM—consists of two parts (Fig. 1). The first is the Bragg mirror, which is grown by metal oxide chemical vapor deposition (MOCVD) with reflection exceeding 99.5%. The second is the active region, including saturable absorber layer with a thickness of 21.4 nm, grown by molecular beam epitaxy at low temperature (400 °C). They are separated by GaAs barriers, placing the quantum well (QW) into the antinode of the standing wave pattern of the laser electric field. Thickness of the absorber layer is sufficiently designed to absorb the incident wavelength.

Figure 2 illustrates the reflection spectrum of this SESAM with a single QW. Based on this figure, it is evident that this structure can be characterized by extremely high reflectivity ($> 90\%$) in the wavelength region of 1010−1110 nm. Meanwhile, the reflectivity bandwidth is wide (∼100 nm), supporting the generation of picosecond or sub-picosecond ultrashort laser pulses. Asymmetry of reflectance spectrum at approximately 1090 nm is caused by two-dimensional (2D) density of states (DOS), which likewise results in asymmetry of the imaginary part of QW's dielectric function around 1090 nm.

Figure 3 illustrates the electric field distribution of the SESAM, which is simulated by an optical software dubbed "Scout". Based on the distribution pattern of standing-wave electric field, the electric field intensity at the InGaAs QW layer can be observed clearly. In Fig. 3,

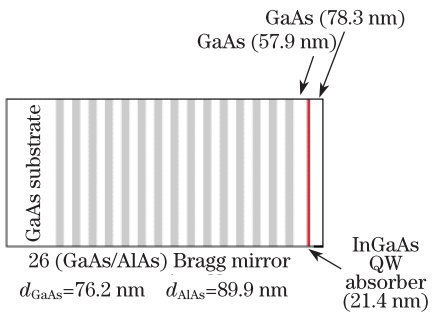

Fig. 1. Structure of the SESAM sample.

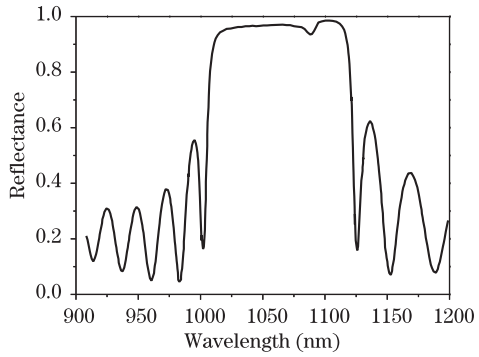

Fig. 2. Reflection spectrum of the SESAM sample.

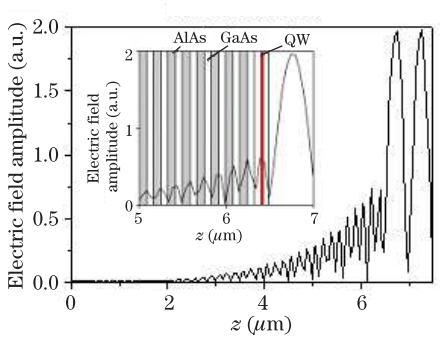

Fig. 3. Electric field distribution in the SESAM.

every vertical line depicts an interface between layers, and the curve represents the electric field amplitude. It is evident that QW is located almost exactly at the peak of electric field. Thus, the absorber can effectively absorb incident light with wavelength of 1090 nm.

Pump-probe technique was deemed the simplest method for ultrafast spectroscopy detection (Fig. 4). The femtosecond pulse was split into two beams. One beam reached the sample as a pump pulse. The other, a probe beam that explored the sample with a variable delay (from femtosecond to microsecond), measured the change in the transmitted probe pulse energy or average power as a function of delay. The excitation pulse altered the sample absorption detected by the probe pulse. The light route of probe beam was modulated by mechanical delay. Figure 5 presents the ultrafast spectra, likewise called dynamic response characteristic of the SESAM, detected using reflection pump-probe technique.

The output laser of femtosecond laser system featured 10-mW output power, 1030-nm wavelength, 80-fs pulse width, and 250-kHz repetition rate (Fig. 4). The output laser was divided into two beams by a splitter. Prior to being split, light energy of pump beam accounted for 80% of the laser energy. The pump beam vertically reached the SESAM sample after being focused by a convex lens; the other beam's energy accounted for 20% of the laser energy before the splitter. The probe beam reached the SESAM sample at a 45° incident angle after passing through stage delay, and was subsequently focused by a convex lens. Probe light was split into two beams by a 50% splitter before being focused by a convex lens. As a reference beam, one beam, with 50% probe energy, was converted into electric signal by a photodiode. Its energy was calculated after the electric signal passed through a data acquisition system and computer. Thus, the reflection of SESAM sample was calculated by the ratio of two light energies detected by two photodiodes.

In establishing the pump-probe system, the pump light spot should be located at the center of probe light spot on the SESAM sample. This should be carried out after being focused by the convex lens, with the help of a pinhole. Subsequently, the shaker, which consisted of two holophotes connected at a 90° angle, was moved back and forth to render optical paths of pump beam and probe beam equal. The pump pulse and probe pulse initially reached the SESAM sample simultaneously. To protect the SESAM from being damaged by high-intensity light, a half-wave plate (HWP) and polarizer were both inserted in the route before the lens. Rotating the polarizer modulated the light energy that reached the sample.

Ultrafast dynamics of the SESAM are detected by the pump-probe setup, pump wavelength, and probe wavelength; the latter two are both 1030 nm. Ultrafast spectra of the SESAM for different excitation fluences are measured and presented in Fig. 5, from which the change of reflection can be observed as a function of pump-probe delay for different pump excitation fluences.

Based on the experiment, it is evident that for the same pulse width, the change of reflection becomes greater when the excitation fluence increases. When the incident light power is 0.5 mW, the ultrafast time constant is 132 fs and the slow time constant is 39.1 ps. As reflectivity changes sensitively in such transient time, it can be concluded that the change of reflectivity is caused by the change of electron density of the conduction band in the semiconductor.

When all carriers in the valence band are excited into the conduction band, indicating the valence band is bleached, the change of reflectivity is maximum. The

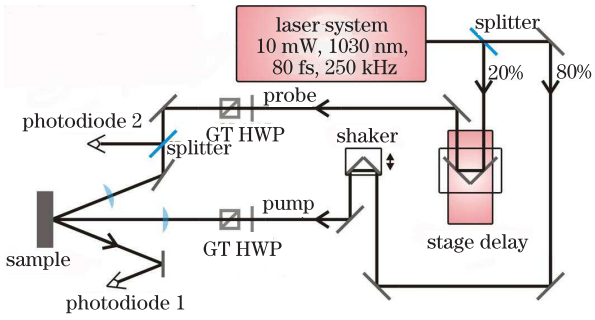

Fig. 4. Pump-probe setup. HWP: half-wave plate; GT: Gran-Thompson polarizer.

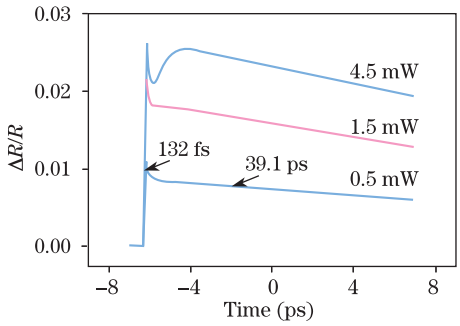

Fig. 5. Change of reflection as a function of pump-probe delay for different pump excitation fluences.

ultrafast time constant is caused by thermal equilibration of carriers in the sub-band of conduction band. Meanwhile, the slow time constant is caused by trapping because of defects and recombination between the valence band and the conduction band. While excitation fluence is maintained sufficiently high to bleach the valence band after the rapid decrease of the change of reflectivity caused by thermal equilibration of carriers in the conduction band, the change of reflectivity again rises for a short period and subsequently decreases slowly. Recovery of rising is caused by cooling of carriers in the conduction band.

In the pump-probe experiment, pump beam and probe beam were focused on the sample by convex lenses. The change of reflection can be measured as a function of the pump-probe delay for different excitation fluences by pump-probe experiment, in which pump and probe pulses can be different colors. The QW is designed at the peak of standing-wave electric field, thus the bleaching process caused by the pump light represents carrier density change in the QW. This is detected by the probe light after a variable delay.

The absorption process of saturable absorber consists of three parts: ultrafast, intermediate, and slow time constants. Ultrafast time constant is caused by thermal equilibration, and it is at the same time scale as the pulse width (< 150 fs) measured by autocorrelator. Intermediate time constant is approximately 1 ps, which is caused by the cooling of carriers in the conduction band. Slow time constant is at the time scale from picosecond to nanosecond, which is caused by carrier trapping resulting from defects induced by lattice deformation of surface. Slow time constant of sample with mismatching lattice is shorter than that of the sample with matching lattice.

Figure 5 presents the ultrafast spectrum of dynamic response for 0.5-mW pumping power, which represents a typical saturable absorber response at low fluence. When the pumping power increases to a certain degree (such as reaching 1.5 or 4.5 mW, as illustrated in Fig. 5), the signal detected by the pump beam will increase nonlinearly. From Fig. 5, we can observe that after the saturation peak and fast recovery time constant resulting from thermal equilibration, a slow bleaching process emerges and continues for approximately 1 ps. The change of reflectivity slowly increases for 1 ps because of the slow bleaching process caused by quasi-Fermi level increasing to above the energy of pump-probe photon. Thus, the slow bleaching process is caused by the cooling of carriers. Carrier relaxation of pseudo-equilibrium results in Fermi distribution of carriers. Fermi distribution is described by two parameters: quasi-Fermi level μ and temperature of carriers T_C. The temperature of carriers T_C is initially higher than the lattice temperature. However, in the following relaxation processes, hot carriers exchange energy with lattice by emitting and absorbing phonon. Thus, energy flows from carriers to lattice. Emission, absorption, and reabsorption of acoustic phonon result in the time scale of relaxation process varying from picoseconds to nanoseconds. When the temperature of hot carriers decreases to that of lattice, the relaxation process ends.

Nonlinear reflectivity of SESAM as a function of excitation fluence is illustrated in Fig. 6. At low excitation fluence, reflectivity increases along with excitation fluence. While the excitation fluence increases to a certain degree, the saturable absorber is saturated and the reflectivity hardly changes. The saturation fluence is the fluence required to increase the reflectivity by $ye \cdot \Delta R$ (37% of ΔR), when incident on the thin absorber. Thus, the saturation fluence of the SESAM in our experiment was 61.2 μJ/cm^2.

From the ultrafast spectrum of the SESAM in Fig. 7, we can observe that at ultrahigh fluence level ($\sim$ 1400 μJ/cm^2), an additional induced absorption component begins to dominate ultrafast nonlinear dynamics. A negative change is observed for positive delays, and the magnitude increases with respect to the square of fluence.

Two-photon absorption (TPA) directly induces the ground state to absorb two photons in order to reach even higher excitation state. Thus, the value of the absorption coefficient can affect reflectance. When the absorption coefficient β increases, the valley bottom of the curve will be deeper. In contrast, when the absorption coefficient β decreases, the valley bottom of the curve will be shallower.

This additional induced absorption can be attributed to free carriers that the TPA creates high in the bands. Partial recovery time constant of this signal indicates that absorption by these highly excited carriers is greater than that of cooler carriers; the relaxation rate from high lying states is slower compared with ordinary carrier cooling.

At high excitation fluences, free carrier absorption (FCA) arising from TPA-generated carriers becomes increasingly important. Initially, hot carriers enhance this FCA. Time-resolved experiments likewise reveal an anomalously slow cooling of a portion of the initial,

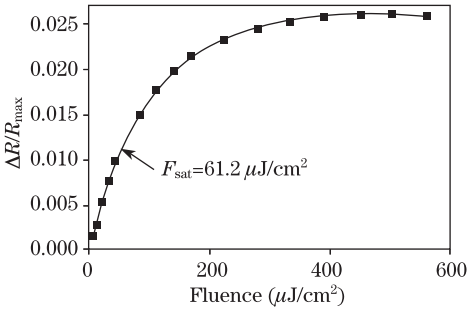

Fig. 6. Nonlinear reflectivity of SESAM versus excitation fluence.

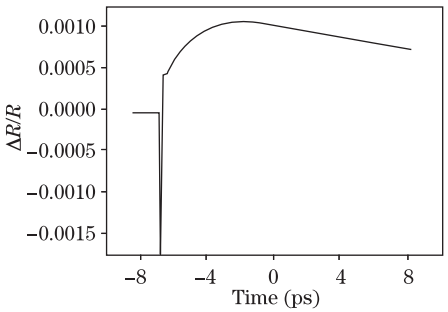

Fig. 7. Nonlinear reflectivity of the SESAM as a function of delay time for high excitation fluence.

highly excited carrier distribution. The corresponding time constant may have implications for pulse shaping in mode-locked lasers using SESAMs.

When a SESAM is exposed to laser, its dynamic response can directly influence pulse shaping of ultrafast laser pulse. Dynamic response or recovery time of the SESAM is measured by a pump-probe setup, from which femtosecond spectroscopy of the SESAM at different excitation fluences, nonlinear reflectivity of the SESAM as a function of excitation fluence, and femtosecond spectroscopy of the SESAM at ultrahigh excitation fluence ($\sim 1400\ \mu J/cm^2$) are measured. When the incident light power increases, nonlinear changes of femtosecond spectroscopy can be observed. TPA can be observed in femtosecond spectroscopy of the SESAM at ultrahigh excitation fluence ($\sim 1400\ \mu J/cm^2$), which may have implications for pulse shaping in mode-locked lasers using SESAMs.

This work was supported by the Ministry of Science, Research, and the Arts of Baden-Württemberg State of Germany and the Chinese Scholarship Council.

References

1. U. Keller, D. A. B. Miller, G. D. Boyd, T. H. Chiu, J. F. Ferguson, and M. T. Asom, Opt. Lett. **17,** 505 (1992).
2. U. Keller, Nature **424,** 831 (2003).
3. L. Huang, J. P. Callan, E. N. Glezer, and E. Mazur, Phys. Rev. Lett. **80,** 185 (1998).
4. K. Herz, G. Bacher, A. Forchel, H. Strsub, G. Brunthaler, W. Faschinger, G. Bauer, and C. Vieu, Phys. Rev. B **59,** 2888 (1999).
5. H. J. Zeiger, J. Vidal, T. K. Cheng, E. P. Ippen, G. Dresselhaus, and M. S. Dresselhaus, Phys. Rev. B **45,** 768 (1992).
6. M. Joschko, P. Langlois, E. R. Thoen, E. M. Koontz, E. P. Ippen, and L. A. Kolodziejski, Appl. Phys. Lett. **76,** 1383 (2000).
7. E. R. Thoen, E. M. Koontz, M. Joschko, P. Langlois, T. R. Schibli, F. X. Kärtner, E. P. Ippen, and L. A. Kolodziejski, Appl. Phys. Lett. **74,** 3927 (1999).
8. P. Langlois, M. Joschko, E. R. Thoen, E. M. Koontz, F. X. Kärtner, E. P. Ippen, and L. A. Kolodziejski, Appl. Phys. Lett. **75,** 3841 (1999).
9. J. Mork, J. Mark, and C. P. Seltzer, Appl. Phys. Lett. **64,** 2206 (1994).
10. D. H. Sutter, I. D. Jung, F. X. Kärtner, N. Matuschek, F. Morier-Genoud, V. Scheuer, M. Tilsch, T. Tschudi, and U. Keller, IEEE J. Sel. Top. Quantum Electron. **4,** 169 (1998).
11. Y. Xue, Q. Liu, L. Chai, Q. Wang, J. Li, and J. Wang, Chinese J. Lasers (in Chinese) **36,** 1937 (2009).
12. X. Li, Y. Wang, S. Zhang, X. Wang, and X. Xu, Acta Opt. Sin. (in Chinese) **29,** 3103 (2009).